Synthetic Aperture Inversion for Arbitrary Flight Paths in the Presence of Noise and Clutter

Birsen Yazici, Ph.D., Rensselaer Polytechnic Institute
Margaret Cheney, Ph.D., Rensselaer Polytechnic Institute

Key Words: SAR, microlocal analysis, arbitrary flight path, noise, clutter

SUMMARY

This paper considers Synthetic Aperture Radar and other synthetic aperture imaging systems from an arbitrary (known) flight path. We assume a single-scattering model for the radar data, and we assume that the ground topography is known but not necessarily flat.

We focus on cases in which the antenna footprint is so large that the standard narrow-beam algorithms are not useful. For this case, [21] gave an explicit backprojection imaging formula that corrects for the ground topography, flight path, antenna beam pattern, source waveform, and other geometrical factors. In this paper, we show how to modify the backprojection algorithm to account for statistical information about noise and clutter.

I. *INTRODUCTION*

In Synthetic Aperture Radar (SAR) imaging [7] [10] [12] [14][25][31], a plane or satellite carrying an antenna moves along a flight path. The antenna emits pulses of electromagnetic radiation, which scatter off the terrain, and the scattered waves are measured with the same antenna. The received signals are then used to produce an image of the terrain. (See Figure 1)

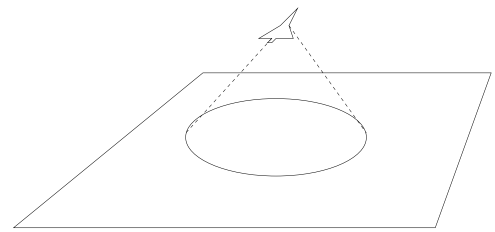

Fig. 1. Acquisition geometry for SAR with an antenna with poor directivity

The nature of the imaging problem depends on the directivity of the antenna. We are interested particularly in the case of antennas with poor directivity, where the antenna footprint is large and standard narrow-beam imaging methods are not useful. This is typically the case for foliage-penetrating radar [30] [31], whose low frequencies do not allow for much beam focusing.

There are two main classes of imaging algorithms, one statistical and the other deterministic. Both approaches encompass many specialized techniques, however, deterministic approaches do not have an explicit mechanism to incorporate statistical information about the scene, noise, or clutter.

Some attempts have been made to develop edge-preserving reconstruction algorithms for SAR [5], [6]. These approaches are typically very computationally intensive. In this paper, we show how statistical information can be incorporated into a class of deterministic imaging algorithms relevant for radar imaging. Our approach has the advantage of providing an algorithm whose computational burden is less severe than that of some other approaches.

The methods we use in this paper are based on microlocal analysis [11] [16] [29], which is a theory for dealing with oscillatory integrals and singularities. These microlocal methods enable us to reconstruct edges and boundaries between different materials in the scattering region [2], [1], [4], [19], [23], [24]. These edges and boundaries correspond mathematically to singularities in the reflectivity function; an image of these singularities gives us an image of structures such as walls and vehicles. The microlocal approach has the advantage of providing reconstruction formulas even in the case when the data are incomplete and non-ideal. In addition, these methods can accommodate the varying antenna beam patterns that arise in the cases of non-ideal antenna motion and gain, and with appropriate adjustments the same reconstruction formulas apply to both spotlight-mode [8] and stripmap-mode radar [12] [14]. Microlocal reconstruction techniques have been used to advantage in the geophysics community, where the resulting algorithms have been found to be fast and robust [2] [4].

Microlocal methods have the limitation that they can only be expected to provide a reconstruction of singularities and their strengths. However, in practice they often reduce to the exact inversion formulas that are known for idealized cases. This is the case here: our reconstruction formula reduces to the exact inversion formula of [13] [17] [20] for the case of a perfect point source moving along a single straight flight track above a flat earth. Furthermore, when there is no noise and clutter; and no statistical information on the target is available, our inversion formula reduces to the deterministic one presented in [21].

The microlocal aapproach leads to generalized *filtered backprojection* algorithms for image reconstruction. In this paper, we show how the filter can be designed to incorporate statistical information about the target, noise and clutter.

The paper is organized as follows. Section 2 introduces the mathematical model and relevant notation. Section 3 develops the image formation algorithm, explains how the filter should be chosen in the generalized filtered backprojection algorithms. Section 4 summarizes our results and conclusion.

We use the capital letters $\boldsymbol{X}$ and $\boldsymbol{Y}$ for spatial variables in $\mathbb{R}^3$, when there is danger of confusion between twodimensional and three-dimensional vectors; the corresponding x and y denote the projections of $\boldsymbol{X}$ and $\boldsymbol{Y}$ onto $\mathbb{R}^2$.

II. *THE MATHEMATICAL MODEL*

For SAR, the correct model is of course Maxwell's equations, but the simpler scalar wave equation is commonly used:

$$\left(\nabla^2 - \frac{1}{c^2(\boldsymbol{X})}\partial_t^2\right) u(t, \boldsymbol{X}) = 0, \tag{1}$$

where c is the wave propagation speed. Each component of the electric and magnetic fields in free space satisfies (1); thus it is a good model for the propagation of electromagnetic waves in dry air.

We assume the earth's surface is located at the position given by $\boldsymbol{X} = \boldsymbol{\psi}(\boldsymbol{x})$, where $\boldsymbol{\psi} : \mathbb{R}^2 \to \mathbb{R}^3$ is known. Because electromagnetic waves are rapidly attenuated in the earth, we assume that the scattering takes place in a thin region near the surface; thus we assume that the perturbation in wave speed c is of the form $c^{-2}(\boldsymbol{X}) - c_0^{-2} = V(\boldsymbol{x})\delta(\boldsymbol{X} - \boldsymbol{\psi}(\boldsymbol{x}))$. Here c_0 is the speed of light in dry air, and V, the *ground reflectivity function*, is the quantity we wish to image.

We show in [22], for the noiseless case, that the received field at sensor location Y and time t can be approximated by the expression

$$S(\boldsymbol{Y}, t) = \iint e^{-i\omega(t-2|\boldsymbol{\psi}(\boldsymbol{x})-\boldsymbol{Y}|/c_0)} W(\boldsymbol{x}, \boldsymbol{Y}, \omega) V(\boldsymbol{x}) d\omega d^2\boldsymbol{x}, \tag{2}$$

where ω denotes the angular frequency; W contains geometrical factors such as the antenna beam pattern and the r^{-2} attenuation from geometrical spreading, and includes also the Fourier transform of the time-domain waveform sent to the sensor. Because this waveform is bandlimited, ultimately we reconstruct band-limited approximations to singularities rather than the actual singularities.

We modify the model (2) in two ways. First, we assume that V is composed of two pieces: $V = \rho_T + \rho_C$, where ρ_T corresponds to a target in which we are interested, and ρ_C corresponds to other scatterers in which we are not interested. Second, we include additive noise n, which models thermal fluctuations in the receiver.

The idealized inverse problem is to determine ρ_T from knowledge of $S+n$ for $t \in (T_1, T_2)$ and for Y on a curve. This curve we parametrize by $\boldsymbol{\gamma} := \{ \boldsymbol{\gamma}(s) : \; s_{\min} < s < s_{\max} \}$. We will write $\boldsymbol{R}_{s,\boldsymbol{x}} = \boldsymbol{\psi}(\boldsymbol{x}) - \boldsymbol{\gamma}(s)$.

The data is $d = S + n$:

$$d(t, s) = F[V](t, s) + n(t, s), \tag{3}$$

where

$$F[V](t, s) = \int e^{-i\omega[t-2|\boldsymbol{R}_{s,\boldsymbol{x}}|/c]} A(\boldsymbol{x}, s, \omega) V(\boldsymbol{x}) \; d^2\boldsymbol{x}. \tag{4}$$

Here $A(\boldsymbol{x}, s, \omega) = W(\boldsymbol{x}, \boldsymbol{\gamma}(s), \omega)$ and $n(t, s)$ denotes the receiver noise.

We make the following assumptions about the statistics. First, we assume that the noise is stationary in the fast time component t and statistically uncorrelated in the slow time component s, so that

$$\int e^{-i\omega t} e^{-i\omega' t'} E[n(t, s)n(t', s')] dt dt' = S_N(\omega, s)\delta(\omega + \omega')\delta(s - s'), \tag{5}$$

where E denotes the expected value. Similarly we write

$$E[\rho_T(\boldsymbol{x})\rho_T(\boldsymbol{x}')] = \mathcal{R}_T(\boldsymbol{x}, \boldsymbol{x}') \tag{6}$$

$$E[\rho_C(\boldsymbol{x})\rho_C(\boldsymbol{x}')] = \mathcal{R}_C(\boldsymbol{x}, \boldsymbol{x}') \tag{7}$$

where we assume

$$\mathcal{R}_T(\boldsymbol{x}, \boldsymbol{x}') = \iint e^{-i\boldsymbol{x}\cdot\boldsymbol{\eta}} e^{i\boldsymbol{x}'\cdot\boldsymbol{\eta}'} S_T(\boldsymbol{\eta}, \boldsymbol{\eta}') d\boldsymbol{\eta} d\boldsymbol{\eta}' \tag{8}$$

$$\mathcal{R}_C(\boldsymbol{x}, \boldsymbol{x}') = \iint e^{-i\boldsymbol{x}\cdot\boldsymbol{\eta}} e^{i\boldsymbol{x}'\cdot\boldsymbol{\eta}'} S_C(\boldsymbol{\eta}, \boldsymbol{\eta}') d\boldsymbol{\eta} d\boldsymbol{\eta}'. \tag{9}$$

In addition, we asssume that the amplitude A of (4) satisfies

$$\sup_{(s,t,\boldsymbol{x})\in K} \; | \; \partial_\omega^\alpha \partial_s^\beta \partial_{x_1}^{\rho_1} \partial_{x_2}^{\rho_2} A(\boldsymbol{x}, s, \omega) \; | \leq C \; (1 + \omega^2)^{(2-|\alpha|)/2} \tag{10}$$

where K is any compact subset of $\mathbb{R}_s \times \mathbb{R}_{\boldsymbol{x}}^2$, and the constant C depends on K, β, δ, ρ_1, and ρ_2. This assumption is needed in order to make various stationary phase calculations hold; in fact this assumption makes the "forward" operator F a Fourier Integral Operator [11], [29], [16]. This assumption is valid, for example, when the source waveform p is a short pulse and the antenna is sufficiently broadband. We note that A can be complex; it can thus be used to model non-ideal antenna behavior such as phase aberrations and frequency-dependent changes in the beam pattern.

III. *IMAGE FORMATION*

We form the image $\tilde{\rho}_T$ by means of a filtered backprojection operator B: we write $\tilde{\rho}_T(\boldsymbol{z}) := Bd(\boldsymbol{z})$, where

$$Bd(\boldsymbol{z}) := \iint Q(\boldsymbol{z}, s, \omega) e^{i\omega[t-2|\boldsymbol{R}_{s,\boldsymbol{z}}|/c]} d(t, s) \; dt ds, \tag{11}$$

where Q is determined below.

To determine Q, we examine below the degree to which the image $\tilde{\rho}_T$ reproduces the true ρ_T, or at least the best approximation to ρ_T we could hope to obtain from our limited data.

The best approximation to ρ_T we can hope for is determined by the flight path and the frequency band of the radar system. In particular, the best mean-square approximation ρ_Ω to ρ_T is

$$\begin{aligned} \rho_\Omega(\boldsymbol{z}) &= I_\Omega \rho_T(\boldsymbol{z}) = \tfrac{1}{(2\pi)^2} \int_{\Omega_{\boldsymbol{z}}} e^{i(\boldsymbol{z}-\boldsymbol{x})\cdot\boldsymbol{\xi}} \rho_T(\boldsymbol{x}) d^2\boldsymbol{x} \\ &= \tfrac{1}{(2\pi)^2} \int e^{i(\boldsymbol{z}-\boldsymbol{x})\cdot\boldsymbol{\xi}} \chi_{\Omega_{\boldsymbol{z}}}(\boldsymbol{x}) \rho_T(\boldsymbol{x}) d^2\boldsymbol{x}, \end{aligned} \tag{12}$$

where $\Omega_{\boldsymbol{z}}$ denotes the set of $\boldsymbol{\xi}$ determined by the flight path and frequency band and where $\chi_{\Omega_{\boldsymbol{z}}}$ is the function that is 1 if $\boldsymbol{x}$ is in the set $\Omega_{\boldsymbol{z}}$ and zero otherwise. We will see below that this set consists of those $\boldsymbol{\xi}$ obtained from (23) as s varies over $[s_{min}, s_{max}]$ and ω varies over the frequency band of the system

A. Determination of the filter Q

We would like to determine the filter Q so that $\tilde{\rho}$ obtained from (11) is as close as possible to ρ_Ω. In particular, we want to determine Q in order to minimize the quantity

$$\Delta(Q) = E\left[\int \left|B\left(F[V]+n\right)(\boldsymbol{z}) - I_\Omega \rho_T(\boldsymbol{z})\right|^2 d^2\boldsymbol{z}\right], \quad (13)$$

where E denotes expected value. The $\boldsymbol{z}$-integral of (13) is simply the L^2-norm, which can be written as the inner product $\langle \cdot, \cdot \rangle$:

$$\begin{aligned}\Delta(Q) &= E\big\langle (BF - I_\Omega)\rho_T + BF\rho_C + Bn, \\ &\quad (BF - I_\Omega)\rho_T + BF\rho_C + Bn\big\rangle \\ &= \Delta_T(Q) + \Delta_C(Q) + \Delta_N(Q), \end{aligned} \quad (14)$$

where

$$\Delta_T(Q) = E\langle (BF - I_\Omega)\rho_T, (BF - I_\Omega)\rho_T\rangle \quad (15)$$

$$\Delta_C(Q) = E\langle BF\rho_C, BF\rho_C\rangle \quad (16)$$

$$\Delta_N(Q) = E\langle Bn, Bn\rangle \quad (17)$$

We note that the cross terms of (14) disappear because we are assuming that the statistics of the target, clutter, and noise are all mutually independent.

1) Simplification of Δ*:* Since the operators $BF - I_\Omega$, BF, and B are integral operators, Δ_T, Δ_C, and Δ_N are each of the form

$$\begin{aligned}\Delta(Q) &= E\langle \mathcal{K}f, \mathcal{K}f\rangle \quad (18) \\ &= E\left[\int \overline{\int K(\boldsymbol{z},\boldsymbol{x}) f(\boldsymbol{x}) d\boldsymbol{x}} \int K(\boldsymbol{z},\boldsymbol{x}') f(\boldsymbol{x}') d\boldsymbol{x}' d\boldsymbol{z}\right] \\ &= \iiint \overline{K(\boldsymbol{z},\boldsymbol{x})} \mathcal{R}_f(\boldsymbol{x},\boldsymbol{x}') K(\boldsymbol{z},\boldsymbol{x}') d\boldsymbol{z} d\boldsymbol{x} d\boldsymbol{x}'\end{aligned}$$

where the bar denotes complex conjugate and $\mathcal{R}_f$ is the autocorrelation function

$$\mathcal{R}_f(\boldsymbol{x},\boldsymbol{x}') = E[\overline{f(\boldsymbol{x})} f(\boldsymbol{x}')] \quad (19)$$

Next we simplify the product BF. The composition of (4) and (11) results in

$$\begin{aligned}BFf(\boldsymbol{z}) = 2\pi \iiint & e^{2ik(|\boldsymbol{R}_{s,\boldsymbol{x}}| - |\boldsymbol{R}_{s,\boldsymbol{z}}|)} Q(z,s,\omega) \\ & \cdot A(\boldsymbol{x},s,\omega) f(\boldsymbol{x}) d\omega ds d^2\boldsymbol{x},\end{aligned} \quad (20)$$

where we have writen $k = \omega/c_0$. We assume that the geometrical conditions on the flight path outlined in [21] for avoiding artifacts are satisfied, so that the leading order contributions to (20) come from the single critical point $\boldsymbol{x} = \boldsymbol{z}$. As in [21], we expand the exponent of the first term of (20) in a Taylor series about $\boldsymbol{x} = \boldsymbol{z}$:

$$2k(|\boldsymbol{R}_{s,\boldsymbol{x}}| - |\boldsymbol{R}_{s,\boldsymbol{z}}|) = -2k(\boldsymbol{z} - \boldsymbol{x}) \cdot \boldsymbol{\Xi}(s,\boldsymbol{x},\boldsymbol{z}) \quad (21)$$

where for $\boldsymbol{x} = \boldsymbol{z}$, we have

$$\boldsymbol{\Xi}(s,\boldsymbol{z},\boldsymbol{z}) = \widehat{\boldsymbol{R}_{s,\boldsymbol{z}}} \cdot D\psi(\boldsymbol{z}) + \ldots, \quad (22)$$

and make the (Stolt) change of variables

$$(s,\omega) \rightarrow \boldsymbol{\xi} = -2k\widehat{R_{s,\boldsymbol{z}}} \cdot D\boldsymbol{\psi}(\boldsymbol{z}). \quad (23)$$

The change of variables (23) transforms the integral (20) into

$$\begin{aligned}BFf(\boldsymbol{z}) &= 2\pi \iint e^{i(\boldsymbol{z}-\boldsymbol{x})\cdot\boldsymbol{\xi}} Q(\boldsymbol{z},s,\omega) A(\boldsymbol{x},s,\omega) \\ &\quad \cdot J(\boldsymbol{z},s,\omega) f(\boldsymbol{x}) d^2\boldsymbol{\xi}\ d^2\boldsymbol{x} + \ldots\end{aligned} \quad (24)$$

where s and ω are understood to refer to $s(\xi)$ and $\omega(\xi)$, respectively, where $J(\boldsymbol{z},s,\omega) = |\partial(s,\omega)/\partial\boldsymbol{\xi}|$, and where the dots indicate remainder terms from higher-order terms of the Taylor expansion. Equation (24) exhibits the operator BF as a pseudodifferential operator. Pseudodifferential operators have the *pseudolocal* property [29], i.e., they do not move singularities or change their orientation. It is this property that ensures that in the no-noise case, the image shows all the visible edges in the scene (i.e., in $\rho_T + \rho_C$).

We apply the above change of variables to the terms Δ_T and Δ_C:

$$\begin{aligned}\Delta_T(Q) &= (2\pi)^2 \int \Big[\iint e^{-i(\boldsymbol{z}-\boldsymbol{x})\cdot\boldsymbol{\xi}} \overline{[Q(\boldsymbol{z},s,\omega)A(\boldsymbol{x},s,\omega)} \\ &\quad \overline{\cdot J(\boldsymbol{z},s,\omega) - \chi_{\Omega_{\boldsymbol{z}}}(\boldsymbol{\xi})]} \mathcal{R}_T(\boldsymbol{x},\boldsymbol{x}') d^2\boldsymbol{\xi}\ d^2\boldsymbol{x} \\ &\quad \iint e^{i(\boldsymbol{z}-\boldsymbol{x}')\cdot\boldsymbol{\xi}'} [Q(\boldsymbol{z},s',\omega')A(\boldsymbol{x}',s',\omega') \\ &\quad \cdot J(\boldsymbol{z},s',\omega') - \chi_{\Omega_{\boldsymbol{z}}}(\boldsymbol{\xi}')] d^2\boldsymbol{\xi}'\ d^2\boldsymbol{x}' \Big] d^2\boldsymbol{z}\end{aligned} \quad (25)$$

$$\begin{aligned}\Delta_C(Q) &= (2\pi)^2 \int \Big[\iint e^{-i(\boldsymbol{z}-\boldsymbol{x})\cdot\boldsymbol{\xi}} \overline{[Q(\boldsymbol{z},s,\omega)A(\boldsymbol{x},s,\omega)} \\ &\quad \overline{\cdot J(\boldsymbol{z},s,\omega)]} \mathcal{R}_C(\boldsymbol{x},\boldsymbol{x}') d^2\boldsymbol{\xi}\ d^2\boldsymbol{x} \\ &\quad \iint e^{i(\boldsymbol{z}-\boldsymbol{x}')\cdot\boldsymbol{\xi}'} [Q(\boldsymbol{z},s',\omega')A(\boldsymbol{x}',s',\omega') \\ &\quad \cdot J(\boldsymbol{z},s',\omega')] d^2\boldsymbol{\xi}'\ d^2\boldsymbol{x}' \Big] d^2\boldsymbol{z}.\end{aligned} \quad (26)$$

In Δ_N we simply use (5):

$$\begin{aligned}\Delta_N(Q) &= \int e^{-i\omega t + 2ik|\boldsymbol{R}_{s,\boldsymbol{z}}|} \overline{Q(\boldsymbol{z},s,\omega)} \mathcal{R}_N(t,s,t',s') \\ &\quad \cdot e^{i\omega' t' - 2ik'|\boldsymbol{R}_{s',\boldsymbol{z}}|} Q(\boldsymbol{z},s',\omega') dt' d\omega' ds' dt d\omega ds d^2\boldsymbol{z} \\ &= \int |Q(\boldsymbol{z},s,\omega)|^2 S_N(\omega,s) ds d\omega d^2\boldsymbol{z}.\end{aligned} \quad (27)$$

We use (8) and (9) in (25) and (26) and then apply the method of stationary phase in the variables $\boldsymbol{x}'$, $\boldsymbol{\xi}'$, $\boldsymbol{x}$, and $\boldsymbol{\xi}$. The phase in question is

$$\phi = \boldsymbol{x}\cdot(\boldsymbol{\xi} - \boldsymbol{\eta}) + \boldsymbol{z}\cdot(\boldsymbol{\xi}' - \boldsymbol{\xi}) + \boldsymbol{x}'\cdot(\boldsymbol{\eta}' - \boldsymbol{\xi}') \quad (28)$$

so the critical conditions are

$$\begin{aligned}0 = \nabla_{\boldsymbol{x}'}\phi &= \boldsymbol{\eta}' - \boldsymbol{\xi}' \\ 0 = \nabla_{\boldsymbol{\xi}'}\phi &= \boldsymbol{z} - \boldsymbol{x}' \\ 0 = \nabla_{\boldsymbol{x}}\phi &= \boldsymbol{\xi} - \boldsymbol{\eta} \\ 0 = \nabla_{\boldsymbol{\xi}}\phi &= \boldsymbol{x} - \boldsymbol{z}\end{aligned} \quad (29)$$

The leading order term of (25) is then

$$\begin{aligned}&\Delta_T(Q) \approx \\ &\iiint e^{i\boldsymbol{z}\cdot(\boldsymbol{\eta}'-\boldsymbol{\eta})} \overline{[Q(\boldsymbol{z},\boldsymbol{\eta})A(\boldsymbol{z},\boldsymbol{\eta})J(\boldsymbol{z},\boldsymbol{\eta}) - \chi_{\Omega_{\boldsymbol{z}}}(\boldsymbol{\eta})]} \\ &S_T(\boldsymbol{\eta},\boldsymbol{\eta}')[Q(\boldsymbol{z},\boldsymbol{\eta}')A(\boldsymbol{z},\boldsymbol{\eta}')J(\boldsymbol{z},\boldsymbol{\eta}') - \chi_{\Omega_{\boldsymbol{z}}}(\boldsymbol{\eta})] d\boldsymbol{\eta} d\boldsymbol{\eta}' d\boldsymbol{z}\end{aligned} \quad (30)$$

where it is understood that $Q(\boldsymbol{z},\boldsymbol{\eta}) = Q(\boldsymbol{z}, s(\boldsymbol{\eta}), \omega(\boldsymbol{\eta}))$, etc. Similarly, the leading order term of (26) is

$$\Delta_C(Q) \approx \iiint e^{i\boldsymbol{z}\cdot(\boldsymbol{\eta}'-\boldsymbol{\eta})}\overline{[Q(\boldsymbol{z},\boldsymbol{\eta})A(\boldsymbol{z},\boldsymbol{\eta})J(\boldsymbol{z},\boldsymbol{\eta})]} \\ S_C(\boldsymbol{\eta},\boldsymbol{\eta}')[Q(\boldsymbol{z},\boldsymbol{\eta}')A(\boldsymbol{z},\boldsymbol{\eta}')J(\boldsymbol{z},\boldsymbol{\eta}')]d\boldsymbol{\eta}d\boldsymbol{\eta}'d\boldsymbol{z} \quad (31)$$

We now assume stationarity:

$$S_T(\boldsymbol{\eta},\boldsymbol{\eta}') = S_T(\eta)\delta(\boldsymbol{\eta}-\boldsymbol{\eta}') \\ S_C(\boldsymbol{\eta},\boldsymbol{\eta}') = S_C(\eta)\delta(\boldsymbol{\eta}-\boldsymbol{\eta}'). \quad (32)$$

This transforms (30) and (31) into

$$\begin{aligned} \Delta_T(Q) &= \iint |[Q(\boldsymbol{z},\boldsymbol{\eta})A(\boldsymbol{z},\boldsymbol{\eta})J(\boldsymbol{z},\boldsymbol{\eta}) - \chi_{\Omega_{\boldsymbol{z}}}(\boldsymbol{\eta})|^2\, d\boldsymbol{z}d\boldsymbol{\eta}, \\ \Delta_C(Q) &= \iint |Q(\boldsymbol{z},\boldsymbol{\eta})A(\boldsymbol{z},\boldsymbol{\eta})J(\boldsymbol{z},\boldsymbol{\eta})|^2\, d\boldsymbol{z}d\boldsymbol{\eta} \quad (33) \end{aligned}$$

We make the change of variables (23) in (27), which gives us

$$\Delta_N(Q) = \iint |Q(\boldsymbol{z},\boldsymbol{\eta})|^2 J(\boldsymbol{z},\boldsymbol{\eta}) S_N(\boldsymbol{\eta}) d\boldsymbol{z}d\boldsymbol{\eta} \quad (34)$$

2) Variational Analysis: We next calculate the variation of Δ with respect to Q:

$$\begin{aligned} 0 &= \left.\frac{d}{d\epsilon}\right|_{\epsilon=0} \Delta(Q+\epsilon q) \\ &= 2\mathrm{Re}\iint \Big(\overline{qAJ}[QAJ-\chi_\Omega]S_T \\ &\quad +\overline{qAJ}[QAJ]S_C + \overline{q}QJS_N\Big) d\boldsymbol{\eta}d\boldsymbol{z} \quad (35) \end{aligned}$$

If the right side of (35) is to be zero for all q, we must have

$$\overline{AJ}[QAJ-\chi_\Omega]S_T + \overline{AJ}QAJS_C + QJS_N = 0 \quad (36)$$

which we can solve for Q:

$$Q = \frac{\chi_\Omega S_T \overline{AJ}}{|A|^2|J|^2[S_T+S_C] + JS_N} \quad (37)$$

This is the filter that should be used in (11).

IV. *CONCLUSIONS*

We have exhibited a filtered backprojection reconstruction formula for SAR imaging from arbitrary (known) flight paths and non-flat (known) earth topography, in the presence of noise and clutter. We have shown that under the assumption of stationarity of the statistics of the target, clutter, and noise, the filter in the backprojection algorithm should be chosen as (37). This filter automatically gives less weight to those frequencies at which the noise and clutter have significant energy.

Since the amplitude A involves the power spectral density of the waveform, the form (37) provides information on how the waveform should be chosen. Exploration of this we leave for the future.

The approach outlined in this paper, in which the backprojection phase is assumed known, is most useful for problems in which the phase itself is subject to only minimal uncertainty and it is the noise and clutter that are limiting features. For such problems, making use of accurate phase information allows us to avoid smoothing in the image; moreover, the visible singularities appear in the correct locations and orientations.

ACKNOWLEDGMENTS

We are grateful to the Air Force Office of Scientific Research[1] for supporting this work under agreements F49620-03-1-0051 and FA9550-04-1-0223.

REFERENCES

[1] G. Beylkin and R. Burridge, "Linearized inverse scattering problems in acoustics and elasticity", Wave Motion 12 (1990) 15–52.

[2] G. Beylkin, "Imaging of discontinuities in the inverse scattering problem by inversion of a causal generalized Radon transform", J. Math. Phys., 26 (1985) 99–108.

[3] N. Bleistein and R.A. Handelsman, Asymptotic Expansions of Integrals, Dover, New York, 1986.

[4] N. Bleistein, J. K. Cohen, and J.W. Stockwell, The Mathematics of Multidimensional Seismic Inversion, Springer, New York, 2000.

[5] Mjdat etin and W. Clem Karl, "Superresolution and edge-preserving reconstruction of complex-valued synthetic aperture radar images," IEEE International Conference on Image Processing, vol. 1, pp. 701-704, Vancouver, Canada, September 2000.

[6] Mjdat etin, W. Clem Karl, and Alan S. Willsky, "Edge-Preserving Image Reconstruction for Coherent Imaging Applications", IEEE International Conference on Image Processing, vol. 2, pp. 481-484, Rochester, New York, September 2002.

[7] J.C. Curlander and R.N. McDonough, Synthetic Aperture Radar, Wiley, New York, 1991.

[8] W. C. Carrar, R. G. Goodman, R. M. Majewski, Spotlight Synthetic Aperture Radar: Signal Processing Algorithms, Artech House, Boston, 1995.

[9] C. Cafforio, C. Prati, and F. Rocca, "SAR data focusing using seismic migration techniques", IEEE Trans. Aerospace and Electronic Systems 27 (1991) 194–206.

[10] L.J. Cutrona, "Synthetic Aperture Radar", in Radar Handbook, second edition, ed. M. Skolnik, McGraw-Hill, New York, 1990.

[11] J.J. Duistermaat, Fourier Integral Operators, Birkhauser, Boston, 1996.

[12] C. Elachi, Spaceborne Radar Remote Sensing: Applications and Techniques, IEEE Press, New York, 1987.

[13] J.A. Fawcett, "Inversion of N-dimensional spherical means, SIAM J. Appl. Math. 45 (1985) 336–341.

[14] G. Franceschetti and R. Lanari, Synthetic Aperture Radar Processing, CRC Press, New York, 1999.

[15] A. Gustavsson, P.-O. Frölind, H. Hellsten, T. Jonsson, B. Larsson, G. Stenström, and L.M.H. Ulander, "Development and operation of the FOA CARABAS HF/VHF-SAR System", Proc. Fourth International Workshop on Radar Polarimetry, July 13-17, 1998, Nantes, France.

[16] A. Grigis and J. Sjöstrand, Microlocal Analysis for Differential Operators: An Introduction, London Mathematical Society Lecture Note Series vol. 196, Cambridge University Press, 1994.

[17] H. Hellsten and L.E. Andersson, "An inverse method for the processing of synthetic aperture radar data", Inverse Problems 3 (1987), 111–124.

[18] H. Hellsten, L.M.H. Ulander, A. Gustavsson, and B. Larsson, "Development of VHF CARABAS II SAR", SPIE Conference Proceedings Vol. 2747 (SPIE, Bellingham, 1996), 48–60.

[19] A. Louis and E.T. Quinto, "Local Tomographic Methods in SONAR", in Surveys on Solution Methods for Inverse Problems, Ed. D. Colton, H. W. Engl, A.K. Louis, J.R. McLaughlin and W. Rundell, Springer Verlag, New York, 2000.

[20] S. Nilsson, "Application of fast backprojection techniques for some inverse problems of integral geometry", Linköping Studies in Science and Technology, Dissertation No. 499 (1997).

[21] C.J. Nolan and M. Cheney, "Synthetic Aperture Inversion for Arbitrary Flight Paths and Non-Flat Topography", IEEE Transactions on Image Processing 12 (Sept. 2003) 1035-1043.

[22] C. J. Nolan and M. Cheney, "Synthetic Aperture Inversion", Inverse Problems, 18 (2002) 221-236.

[1]Consequently the U.S. Government is authorized to reproduce and distribute reprints for Governmental purposes notwithstanding any copyright notation thereon. The views and conclusions contained herein are those of the authors and should not be interpreted as necessarily representing the official policies or endorsements, either expressed or implied, of the Air Force Research Laboratory or the U.S. Government.

[23] C. J. Nolan and W. W. Symes, "Global solution of a linearized inverse problem for the acoustic wave equation", Comm. in P.D.E., Vol. 22, Nos 5-6, 1997.

[24] E.T. Quinto, "Singularities of the X-ray transform and limited data tomography in R^2 and R^3", SIAM J. Math. Anal., 24(1993), 1215-1225.

[25] M. Soumekh, Synthetic Aperture Radar Signal Processing with MATLAB Algorithms, Wiley, New York, 1999.

[26] M. Soumekh, "Wavefront-based synthetic aperture radar signal processing", Frequenz 55 (2001) 99–113.

[27] M. Soumekh, D. Nobels, M. Wicks, and G. Genello, "Signal processing of wide-bandwidth and wide-beamwidth P-3 SAR data", IEEE Trans. on Aerospace and Electronic Systems 37 (2001) 1122-1141.

[28] F. Treves, Basic Linear Partial Differential Equations, Academic Press, New York, 1975.

[29] F. Treves, Introduction to Pseudodifferential and Fourier Integral Operators, volumes I and II, Plenum Press, New York, 1980.

[30] L.M.H. Ulander and P.-O. Frölund, "Ultra-wideband SAR interferometry", IEEE Trans. on Geoscience and Remote Sensing, vol. 36 no. 5, September 1998, 1540–1550.

[31] L.M.H. Ulander and H. Hellsten, "Low-frequency ultra-wideband array-antenna SAR for stationary and moving target imaging", conference proceedings for the SPIE 13th Annual International Symposium on Aerosense, Orlando, Florida, April 1999.

[32] D.R. Wehner, High-Resolution Radar, second edition, Artech House, Norwood, MA, 1995.